HAYATI
Journal of Biosciences

Vol. 29 No. 2, March 2022 222-233
DOI:10.4308/hjb.29.2.222-233
ISSN: 1978-3019
EISSN: 2086-4094

Intra- and Interspecies Wing Venation Variations of *Apis cerana* and *Apis nigrocincta* Species in Indonesia

Nisfia Rakhmatun Nisa[1], Berry Juliandi[1], Rika Raffiudin[1*], J Jauharlina[2], Mahardika Gama Pradana[3], Araz Meilin[4], J Jasmi[5], Yulia Pujiastuti[6], Puji Lestari[7], Fahri Fahri[8], Windra Priawandiputra[1], Tri Atmowidi[1]

[1]*Department of Biology, Faculty of Mathematics and Natural Science, IPB University, Bogor, Indonesia*
[2]*Department of Plant Protection, Faculty of Agriculture, Universitas Syiah Kuala, Banda Aceh, Indonesia*
[3]*Indonesian Oil Palm Research Institute, Medan, Indonesia*
[4]*Assessment Institute for Agricultural Technology Jambi, Jambi, Indonesia*
[5]*Study Program Industrial Hygiene and Occupational Safety and Health, College of Health Sciences, Padang, Indonesia*
[6]*Department of Plant Protection, Faculty of Agriculture, Sriwijaya University, Palembang, Indonesia*
[7]*Department of Plant Protection, Faculty of Agriculture, Lampung University, Bandar Lampung, Indonesia*
[8]*Department of Biology, Faculty of Mathematics and Natural Sciences, Tadulako University, Palu, Indonesia*

ARTICLE INFO

Article history:
Received September 17, 2021
Received in revised form October 18, 2021
Accepted November 9, 2021

KEYWORDS:
Apidae,
Cubital index,
Geometric Morphometric,
Landmark,
Sundaland,
Wallacea

ABSTRACT

***Apis cerana* has a wide distribution in Asia, including Sundaland, and is currently found in Wallacea, while the sister species, *A. nigrocincta*, is native in Sulawesi. The wide geographic distribution and the island isolation led to form morphological differences in the bees. The morph and wing venations are known to have a high genetic inheritance. Therefore, this research aimed to (1) analyze the landmark variation of wing venations of *A. cerana* from Sundaland and Wallacea, and *A. nigrocincta* from Sulawesi, (2) determine the relationship between these two bee species. The research was conducted by digitizing 550 wing venations based on nineteen landmarks. Our study on intraspecies showed that *A. cerana* Sumatra revealed a high variation in bending energy. Overall, the deformation grid of *A. cerana* from Sundaland has higher displacement than those from Wallacea, meaning higher variations of the Sundaland *A. cerana*. We found geometric morphometric markers of landmarks 16 and 17 in intraspecies and interspecies bees. Thus, these landmarks known as a cubital index can be used for species identification. The differentiation of interspecies has been shown in the PCA. *Apis nigrocincta* was separated from the single group of the centroid *A. cerana* and was supported by the Neighbor-Joining tree.**

1. Introduction

The Asian cavity-nesting honey bees, *Apis cerana*, is distributed in Asia encompass the northern in Ussuria, central Afghanistan, north of Pakistan through northwest India, across southern Tibet, north Myanmar, to East Asia including China, then north-easterly into Korea, Rusia, Japan, and Southeast Asia, from the Malay Peninsula to the Philippines, Celebes, and Timor-Leste (Ruttner 1988; Radloff *et al.* 2010). In Indonesia *A. cerana* was established in Java, Lombok, Bali, Flores, Sulawesi (Damus and Otis 1997), and Sumatra (Engel 1999). This Asian honey bee is currently found in the Moluccas and Papua (Raffiudin *et al.* 2021). Based on morphological structure, several subspecies of *A. cerana* were identified, i.e., *A. c. cerana, A. c. indica, A. c. japonica, A. c. javana*, *A. c. johni*, etc (Engel 1999).

Wing venation has been used for subspecies determination for honey bee *A. mellifera caucasica, A. m. carnica*, and *A. m. mellifera* by applying the geometric morphometrics approach based on eighteen landmarks of the wing venations (Tofilski 2008). An intensive geometric morphometric analysis was also used to *A. cerana* wing venations based on 20 landmarks (Ji *et al.* 2020). They succeeded to separate eight populations of *A. cerana* groups with 95% signification from Central China, Malay (Sabah), Northeast Asia (Heilongjiang and Jilin in China, North Korea, South Korea, and Japan), Hainan (Hainan Island and Yongxing Island), Aba (Maerkang and Jinchuan), Taiwan, Qinghai, and Bomi (South-eastern Tibet). Moreover, in China, *A. cerana* at different temperate and altitudes showed significantly different for the 18 landmark wing venations by applying the

* Corresponding Author
E-mail Address: rika.raffiudin@apps.ipb.ac.id

geometric morphometric analysis (Zhou *et al.* 2016). Larger morphological sizes of *A. cerana* than those in the lowlands of Java (Indonesia) were also found by using the traditional morphometrics approach (Raffiudin *et al.*1999).

In contrast with the wide distribution of *A. cerana*, the other Asian cavity-nesting honey bees, *Apis nigrocincta*, is native in Sulawesi, Mindanao, Sangihe, and small surrounding islands (Otis 1996; Damus and Otis 1997). In Sulawesi, *A. nigrocincta* and *A. cerana* live as sympatric species (Hadisoesilo *et al.* 1995). The traditional morphometric analysis based on 18 morphological characters were successfully separated those two honey bee species (Damus and Otis 1997). Both have been confirmed as sister taxon based on molecular analysis (Raffiudin and Crozier 2007). However, there is a lack of information regarding the geometric morphometric analysis of the wing venations comparing these two sympatric species in Sulawesi in the same environmental condition.

Therefore, we aimed to analyze the variation of wing venation landmarks in the: (1) intraspecies of *A. cerana* from Indonesian archipelagos, i.e., Sumatra, Belitung, Java, Bali, Sulawesi, and the Moluccas, and (2) interspecies between *A. cerana* and *A. nigrocincta* in Central Sulawesi, then to clarify the relationship of the two species based on landmarks wing venation.

2. Materials and Methods

2.1. Samples Collection

The bee worker samples used for geometric morphometric analysis were collected from several islands in the Indonesian archipelagos, i.e., 50 colonies of *A. cerana* and five colonies of *A. nigrocincta* (a total of 550 individuals as shown in Table 1). Bee

Table 1. Locations and samples of *A. cerana* and *A. nigrocincta*

Colony ID	Locations	Coordinates	Collectors*
Apis cerana			
A. Sumatra			
Ac1_PnB_AcB_SMT Ac2_PnB_AcB_SMT	Peukan Bada, Aceh	S 5°32'28.43.6" E 95°13'39.85.7"	JHL, TAF, KFH
Ac3_Bkt_BnM_SMT Ac4_Bkt_BnM_SMT	Bukit, Aceh	S 4°42'29.76.4" E 96°51'46.098"	JHL, AFY, MDS
Ac5_SlL_Ash_SMT Ac6_SlL_Ash_SMT	Silo Lama, North Sumatra	S 3°6'24.327" E 99°43'20.003"	MGP, GNS, MRN
Ac7_StS_Pmt_SMT Ac8_StS_Pmt_SMT	Siantar Sitalasati, North Sumatra	N 2°56'31.131" E 99°2'25.792"	MGP, GNS, AHS
Ac9_Krj_PkB_SMT Ac10_Krj_PkB_SMT	Kerajaan, North Sumatra	N 2°40'17.269" E 98°19'37.254"	MGP, GNS, JMS
Ac11_KlJ_TJT_SMT Ac12_KlJ_TJT_SMT	Kuala Jambi, Jambi	S '-1°2'39,40.4" E 103°47'33,9"	AMN, CLA, MRD
Ac13_GnK_Krc_SMT Ac14_GnK_KrC_SMT	Kerinci Mounth, Jambi	S '-1°54'51,009" E 101°14'15,181"	AMN, CLA, JKR
Ac15_SnG_PdP_SMT Ac16_SnG_PdP_SMT	Padang Pariaman, Padang	S '-0°25'37,468" E 100°4'34,172"	JSI, BYC, YAS
Ac17_Btp_TnD_SMT Ac18_Btp_TnD_SMT	Tanah Datar, Padang	S '-0°26'16,028" E 100o26'47,425"	JSI, ZZI, FHI
Ac19_BTS_MsR_SMT Ac20_BTS_MsR_SMT	Bulan Tengah Suku Ulu, South Sumatra	S '-3°23'13,338" E 103°21'40,788"	YPI, ASI, HSO
Ac21_GnM_MrN_SMT Ac22_GnM_MrN_SMT	Mounth Megang, South Sumatra	S '-3°32'6,008" E 103°57'4,267"	YPI, ASI, SYN
Ac23_SdL_MrN_SMT Ac24_SdL_MrN_SMT	Semendo Darat Laut, South Sumatra	S '-4o4'19,853" E 103°38'56,021"	YPI, ASI, TKO
Ac25_Jbg_LmT_SMT Ac26_Jbg_LmT_SMT	Jabung, Lampung	S '-5°19'17,551" E 103°59'56,61"	PLI, DAAR, SYO
Ac27_PrS_PsB_SMT Ac28_PrS_PsBSMT	South Pesisir, Lampung	S '-5°25'17,454" E 105°42'24,632"	PLI, DAAR, SHM
Ac29_WyR_Psw_SMT Ac30_WyR_Psw_SMT	Way Rate, Lampung	S '-5°33'9,156" E 105°6'12,531"	PLI, DAAR, YSA

Table 1. Continued

	Colony ID	Locations	Coordinates	Collectors*
B. Belitung Island				
	Ac1_Kcp_Sjk_BLT Ac2_Kcp_Sjk_BLT	Sijuk, Belitung	S 02° 34,071' E 107° 42'06.5'	RIR, NIS
C. Java				
	Ac1_MkJ_Pndg_Java Ac2_MkJ_Pndg_Java	Pandeglang, Banten	S 06° 23'97.0'' E 106° 04'46.1''	IS, JR
	Ac3_Lbk_Java Ac4_Lbk_Java	Lebak, Banten	S 06° 51'33.2" E 106° 06'02.0"	MT
	Ac5_Ppj_Bgr_Java	Bogor, West Java	S 06° 25'47.0" E 106° 31' 36.3"	AU, YA, SYW, TS, DL
	Ac6_Ppj_Bgr_Java	Bogor, West Java	S 06° 25'47.0" E 106° 31'36.3"	NIS, AA, TS
	Ac7_Nlr_DIY_Java	Mounth Kidul, Special Region of Yogyakarta	S 07° 51'51.9'' E 110° 36'52.1''	HP, WST
	Ac8_Igr_DIY_Java	Bantul, Special Region of Yogyakarta	S 07° 57'34.8'' E 110° 23'29.2''	HP, HTY
D. Bali Island				
	Ac1_Mly_Jbn_Bali Ac2_Mly_Jbn_Bali	Jembrana, Bali	S 08° 15'04.3'' E 114° 29'45.9''	RIR, NIS, MTL, RTH
E. Sulawesi				
	Ac1_JnK_Prg_SLW Ac2_JnK_Prg_SLW Ac3_JnK_Prg_SLW	Jono kalora village, Central Sulawesi	S' 00˚ 47'30.0", E 120˚ 07'51.4"	NIS, FH, KSR, IR
	Ac4_Dlg_Prg_SLW Ac5_Dlg_Prg_SLW Ac6_Dlg_Prg_SLW	Dolago village, Central Sulawe	S' 00˚ 52' 36.4", E 120˚12'36.8"	NIS, NHR
F. Moluccas				
	Ac1_Pka_TlA_AMB Ac2_Pka_TlA_AMB	Poka Village, Ambon	S 03° 39'09.6'' E 128°11' 43.9''	JL, YA
Apis nigrocincta Sulawesi				
	An1_Sgi_SLW An2_Sgi_SLW An3_Sgi_SLW An4_Sgi_SLW	Sigi, Central Sulawesi	S 01° 05'48.12'' E 119°59'22.5''	FHR, SDM, EM
	An5_Prg_SLW	Parigi Moutong, Central Sulawesi	S 00˚ 47' 28.5" E 120˚ 07' 59.3"	NIS, SB, IR

Total colonies = 55

Colony ID Ac: *Apis cerana*, An: *Apis nigrocincta*, Pbd: Peukan Bada, Bkt: Bukit, Sll: Silo laut, Stl: Siantar Sitalasati, Krj: Kerajaan, Klj: Kuala Jambi, Krc: Gunung Kerinci, Pdp: Padang Pariaman, Tnd: Tanah Datar, Btsu: Bulan Tengah Suku Ulu, Gnm: Gunung Megang, Sdl: Semendo Darat Laut, Jbg: Jabung, Prs: South Pesisir, Wrt: Way Rate, Pndg: Pandeglang, Lbk: Lebak, Bgr: Bogor, DIY: Daerah Istimewa Yogyakarta, Jbn: jembrana, Kcp: Keciput Village, Jnk: Jono Kalora, Dlg: Dolago, Sgi: Sigi, Prg: Parigi. Collectors AA: Achmad Alfiyan, AH: Aam Hasanudin AFY: Afriyani, AM: Araz Meilin, ASI: Arsi, AU: Adeliani Ulfie, BYC: Buti Yohenda, Christy, CL: Chandra Lela, DL: Dela, DAAR: Denny Achmad Akbar Roswandi, EM: Evans Madiyono, FHI: Fahmi, FHR: Fahri, GNS: Ganesa, HP: Hari Purwanto, HRN: Hartono, HS: Heru Supriyanto, IR: Ira, IS: Irma Syofyanti, JL: Jacobus SA Lamerkabel, JHL: Jauharlina, JSI: Jasmi, JR: Jenny Rahmadini, JR: Joko Rasmono, JMS: Julkermin Simanjuntak, KSR: Kasiran, KFH: Khairil Fatah, MGP: Mahardika Gama Pradana, MRN: Marmin, MD: Muhammad Darussalam, MTL: Matal, MT: Mita, MRD: Mursyid, NIS: Nurul Insani Shullia, PLI: Puji Lestari, RIR: Rika Raffiudin, RTH: Ratih, SB: Sri Bening, SDM: Sudarmin, SHR: Sahori, SHM: Suherman, SYO: Suyarto, SYN: Suryadin, SYW: Sri Yuliasih Wiyati, TAF: Teuku Andrio Febrian, TKO: Tukino, TS: Tiara Sayusti, WST: Wasito, YA: Yofian Anaktoty, YAS: Yance Andrianus, YPI: Yulia Pujiastuti, YSA: Yayat Supriatna ZZI: Zamzami

samples were paralyzed and preserved by using 70% ethanol.

2.2. Digitization of Wing Landmark

The ten right forewings of the bees per colony were dissected (Rattanawannee *et al.* 2010), photographed, and observed by using Olympus SZ61 stereomicroscope equipped with Optilabviewer2.2. All wing photographs were taken in a consistent position to provide precise digitations. The photographs of the bee wing venations were analyzed using Thin Plate Splin software and digitized three times by tpsDig232 software (Rohlf 2015; https://life.bio.sunysb.edu/morph/) based on 19 landmarks (Figure 1, Table 2) (Michener 2007).

2.3. Geometric Morphometrics Analysis

The honey bee wing venations were analyzed using the Thin Plate Spline (TPS) software. Three landmark replications for the X and Y coordinates of wing venations were aligned using tpsRelw32 to obtain the mean or reference landmarks. Those references were aligned with the average digitization values of the ten bees from each colony (Rohlf *et al.* 1996; Rohlf 2015). Besides the reference landmark, the other two outputs of tpsRelw were: (1) the landmark contribution value and (2) the variance of landmark (S^2). The first landmark contribution and variance landmark values were analyzed for the wing venations *A. cerana* Sumatra samples that comprised 60% out of all samples. The second relative contribution values were analyzed for all *A. cerana* and *A. nigrocincta* samples.

These results were further analyzed using tpsSplin to determine the diversity of wing venation and produce a deformation grid based on the Procrustes Superimposition method (Rohlf and Slice 1990; Rohlf 2004; https://life.bio.sunysb.edu/morph/). Three deformation grids were constructed using tpsSplin: (1) intraspecies of 50 colonies *A. cerana* (aligned with the mean landmarks of the total 500 samples), (2) intraspecies of *A. cerana* and intraspecies of *A. nigrocincta* (the mean wing venation landmarks from each island were aligned to individuals of the respective islands), (3) interspecies of 500 individuals of *A. cerana* that were aligned to the mean landmark of *A. nigrocincta*; and vice versa.

Using tpsSplin (Rohlf 2004; https://life.bio.sunysb.edu/morph/), landmark displacements in the deformation grid of the bee wing venations were analyzed for the bending energy values. Bending energy was defined as the shape deformation value of the landmark configuration (Zelditch 2004). Three bending energy data were constructed, i.e., the bending energy of (1) intraspecies of *A. cerana* wing venations from Sumatra that aligned to all *A. cerana* Sumatra (2) the intraspecies of *A. cerana* from each island that aligned to all individuals *A. cerana* from the six islands, and (3) the interspecies of *A. cerana* and *A. nigrocincta* mean landmarks that aligned with both species wing venations samples.

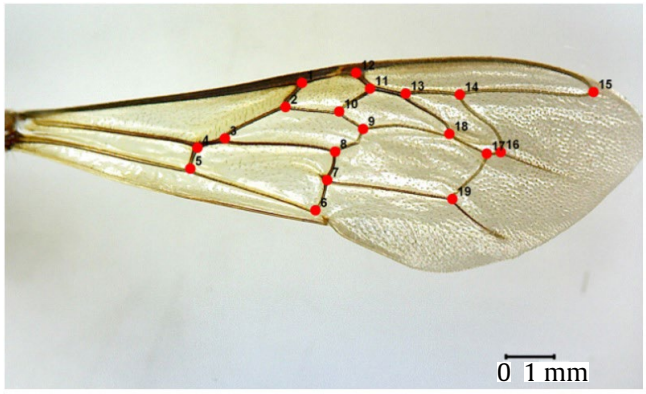

Figure 1. Landmark anatomical points of *A. cerana* and *A. nigrocincta*

Table 2. Description of the wing landmark of the *A. cerana* and *A. nigrocincta* (Michener 2007)

Landmark	Description*
1	Rs and prestigma junctions
2	The point Rs + M
3	Point M + Cu1
4	Point M + Cu2
5	Cu-v point
6	V and Cu2 junctions
7	The vein junctions of Cu1 and Cu2
8	Point 1m-cu
9	Point 2m-cu
10	The second vein junctions of Rs + m and arbiscissa is Rs
11	Arbiscissa junctions both Rs and Rs
12	The junctions of r and stigma
13	Rs and 1r-m junctions
14	Rs and 2r-m junctions
15	The tip point of Rs
16	2r-m point
17	End point 2m-cu
18	1r-m point
19	2m-cu and Cu1 junction

*1m-cu, medio-cubital opposite the first vein; 2m-cu, medio-cubital across the second vein; 1r-m, radio-medial cross-first vein (cross-second submarginal vein); 2r-m, radio-medial opposite-second vein (third submarginal vein); C, costa; Cu, cubitus; Cu1, the first branch of the cubitus; Cu2, second branch cubitus; M, medium (basal vein); r, radial cross-vein; r, radius; R1, the first branch of the radius; Rs, radial sector (Michener 2007)

2.4. Principal Component Analysis (PCA) and Neighbor-Joining Tree Construction

Principal Component Analysis (PCA) used the two highest relative warps (RW) scores that reflect the displacements of landmarks coordinate of the wing venations from each sample using the tpsRelw32

(Rohlf 1993). Further, those values were used to construct the rooted Neighbor-Joining (NJ) tree implemented in the Phylogenetics and Evolution (APE) analysis package (Paradis *et al.* 2004) with the R software (R Core Team 2018). The unrooted NJ tree was constructed for interspecies relationships based on six islands of *A. cerana* and *A. nigrocincta*.

3. Results

3.1. Landmark Variations of *A. cerana* Sumatra

A total of 60% sample of *A. cerana* used in this study was derived from several Sumatra provinces (Aceh, North Sumatra, Jambi, West Sumatra, South Sumatra, and Lampung) (Table 1). Those samples revealed the displacement of landmark wing venation based on 19 landmarks (Table 2), and landmark numbers 11, 16, and 17 showed the three highest contribution values (Table 3A). Therefore, those three landmarks can differentiate the intraspecies *A. cerana* of Sumatra (Table 3A). We also found that the displacement of landmark points affected the different wing shapes (Figure 2A). Another interesting result was shown that the landmark wing venation number 10 also showed a high contribution in *A. cerana* from Aceh, North Sumatra, and West Sumatra (Table 3B).

A deformation grid analysis was conducted to compare the different wing shapes of *A. cerana* Sumatra to all *A. cerana* Indonesia and revealed

Table 3A. Landmark contribution value of *A. cerana* from Sumatra (30 colonies)

Landmark	Contribution value	S^2
1	0.03709	0.00001315
2	0.03636	0.00000851
3	0.02289	0.00000640
4	0.05283	0.00001232
5	0.02064	0.00001944*
6	0.01404	0.00001403
7	0.06063	0.00001328
8	0.06174	0.00000656
9	0.03896	0.00000917
10	0.04965	0.00001241
11	0.13093*	0.00000685
12	0.05956	0.00001008
13	0.03118	0.00000717
14	0.00864	0.00001534*
15	0.00032	0.00002880*
16	0.13753*	0.00001303
17	0.20914*	0.00000851
18	0.02588	0.00001299
19	0.00199	0.00001243

*The most contribution and variation of landmarks values with high variations

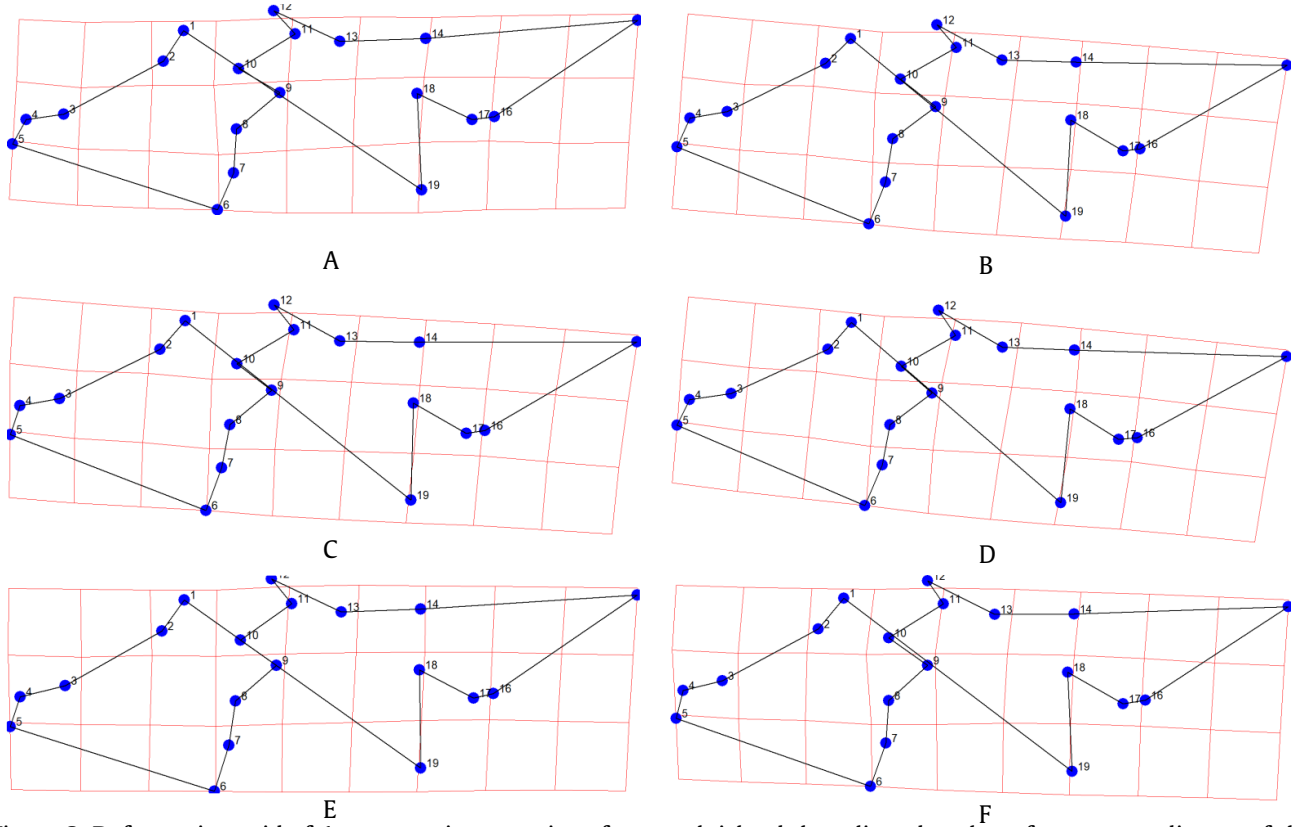

Figure 2. Deformation grid of *A. cerana* wing venations from each island that aligned to the reference coordinates of the total 500 samples *A. cerana* Sundaland: Sumatra (A), Belitung (B), Java (C), Bali (D), *A. cerana* Wallacea from Sulawesi (E), and from Moluccas (F). Note: the straight and unbent grid refers to the same shape to reference a landmark. The more bending to the box indicates the sample has a more different shape to the reference

Table 3B. Landmark contribution values of *A. cerana* from Aceh, North Sumatra and West Sumatra

Landmark	Aceh	North Sumatra	West Sumatra
	Contribution value		
1	0.05094	0.06670	0.01754
2	0.03775	0.05984	0.01461
3	0.01587	0.08751	0.06327
4	0.06395	0.09941	0.08876
5	0.02613	0.01781	0.01762
6	0.02472	0.00848	0.00760
7	0.08039	0.03801	0.01876
8	0.04488	0.03560	0.01685
9	0.13512*	0.06152	0.03135
10	0.14965*	0.10703*	0.11587*
11	0.03354	0.08715*	0.04164
12	0.03590	0.04684	0.00968
13	0.00971	0.05399	0.02510
14	0.00397	0.01147	0.01680
15	0.00027	0.00063	0.00084
16	0.09817	0.08109	0.19941*
17	0.15697*	0.10052*	0.27733*
18	0.03100	0.03212	0.03401
19	0.00106	0.00428	0.00295

*The most contribution and variation of landmarks values with high variations

that landmarks 3, 4, and 5 change the curve of the deformation grid (Figure 2A). This result supports that the bending energy value influenced the deformation grid (Rohlf and Slice 1990). Moreover, *A. cerana* Sumatra has a similar wing shape to *A. cerana* Belitung based on the alignment to each island. Thus, those three landmarks show more differences in these two islands compared to the other islands (Figure 3A and B). This study also found that the mean value of bending energy in the lowland *A. cerana* North Sumatra and Jambi showed higher values than the highland bees (Table 4). Overall, the *A. cerana* Sumatra revealed the highest bending energy value compared to 50 colonies of *A. cerana* from the other islands (Table 5).

In the PCA plot, *A. cerana* Sumatra was distributed at the centroid, except several Sumatra samples that were separate at quadrant 2 and 3 (Figure 4, the square boxes). This separate sample in the PCA plot is supported by the NJ tree of the *A. cerana* ID No Ac20_BTS_MsR_SMT, which has a longer branch than the others (Figure 5).

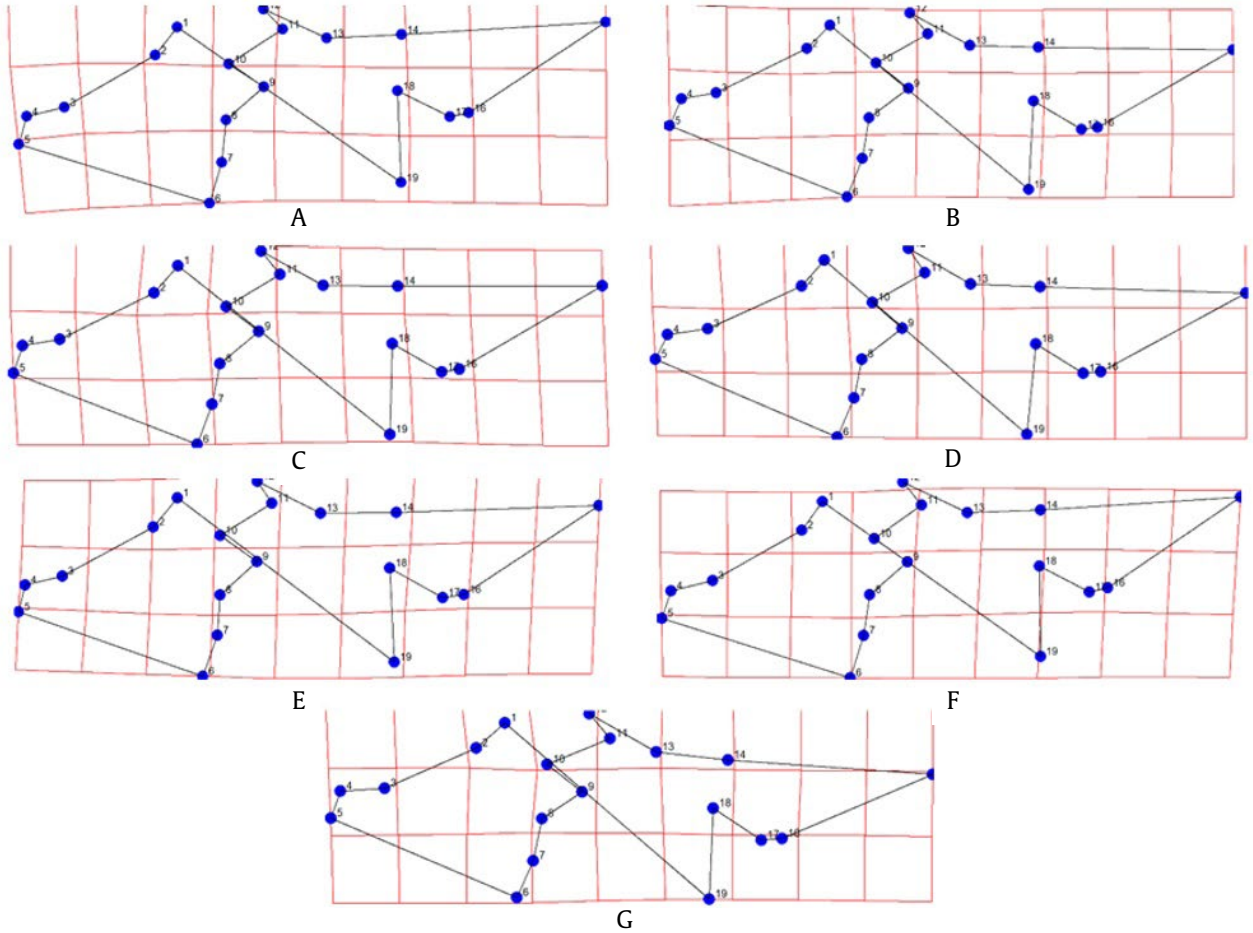

Figure 3. Deformation grid of *A. cerana* and *A. nigrocincta* wing venation derived from mean landmark were aligned to individuals from each island. *A. cerana* Sumatra (A), Belitung (B), Java (C), Bali (D), Sulawesi (E), Moluccas (F), and *A. nigrocincta* Sulawesi (G). Note: the straight and unbent grid refers to the same shape to reference a landmark. The more bending to the box indicates the sample has more different shape to the reference

Table 4. Bending energy of *A. cerana* wing venations from Sumatra in different latitude

Province	Latitude	Colony ID	Bending energy	Bending energy
Aceh	Lowland (Aceh Besar)	Ac1_PnB_AcB_SMT	0.01899	0.02902±0.01003
		Ac2_PnB_AcB_SMT	0.03905	
	Highland (Bener Meriah)	Ac3_Bkt_BnM_SMT	0.01272	0.02417±0.01145
		Ac4_Bkt_BnM_SMT	0.03562	
North Sumatra	Lowland (Silo Lama)	Ac5_SlL_Ash_SMT	0.02950	
		Ac6_SlL_Ash_SMT	0.01173	0.02048±0.02048
	Lowland (Siantar Sitalasati)	Ac7_StS_Pmt_SMT	0.01643	
		Ac8_StS_Pmt_SMT	0.02426	
	Highland (Kerajaan)	Ac9_Krj_PkB_SMT	0.01704	0.01573±0.001315
		Ac10_Krj_PkB_SMT	0.01441	
Jambi	Low Land (Kuala Jambi)	Ac11_KlJ_TJT_SMT	0.03938	0.02434±0.01504
		Ac12_KlJ_TJT_SMT	0.00930	
	Highland (Kerinci)	Ac13_GnK_Krc_SMT	0.01174	0.01148±0.000265
		Ac14_GnK_Krc_SMT	0.01121	
West Sumatra	Lowland (Padang Pariaman)	Ac15_SnG_PdP_SMT	0.01240	0.00922±0.003185
		Ac16_SnG_PdP_SMT	0.00603	
	Highland (Tanah Datar)	Ac17_Btp_TnD_SMT	0.01466	0.01260±0.002065
		Ac18_Btp_TnD_SMT	0.01053	
South Sumatra	Lowland (Musi Rawas)	Ac19_BTS_MsR_SMT	0.00927	
		Ac20_BTS_MsR_SMT	0.05082	0.03005±0.020775
	Highland (Megang Mountain)	Ac21_GnM_MrN_SMT	0.04796	
		Ac22_GnM_MrN_SMT	0.02430	
	Highland (Semendo Darat Laut)	Ac23_SdL_MrN_SMT	0.03192	0.02929±0.012715
		Ac24_SdL_MrN_SMT	0.01297	
Lampung	Lowland (Jabung)	Ac25_Jbg_LmT_SMT	0.00638	
		Ac26_Jbg_LmT_SMT	0.01950	0.01560±0.005483
	Lowland (South Pesisir)	Ac27_PrS_PsB_SMT	0.01656	
		Ac28_PrS_PsBSMT	0.01997	
	Highland (Pesawaran)	Ac29_WyR_Psw_SMT	0.01899	0.01468±0.00431
		Ac30_WyR_Psw_SMT	001037	

Table 5. Bending energy and procrustes distance values *A. cerana* in each island aligned to all *A. cerana* from the six islands

Species	Islands	Bending energies	Procrustes distance (d)
A. cerana	Sumatra	0.03970	0.03970
	Belitung	0.03030	0.03030
	Java	0.02158	0.02158
	Bali	0.02272	0.02272
	Sulawesi	0.01167	0.01167
	Moluccas	0.02083	0.02083

3.2. Intraspecies Variations of *A. cerana* and Interspecies Variation with *A. nigrocincta* Based on Landmark Deformation Grid

The landmark deformation grid of *A. cerana* that aligned to all colonies of *A. cerana* in four islands, Sumatra, Belitung, Java, and Bali, showed high displacement in the nine landmarks number 11-19 (Figure 2 A-D), which were resulted in the high bending energy (Table 5). Interestingly, the bending energy values from *A. cerana* wing venation in Sulawesi and Moluccas are low (Table 5), producing a similar shape to the reference landmarks (Figure 2 E-F).

The deformation grid aligned to each island showed that *A. cerana* from Java, Bali, and Sulawesi did not show a different shape and had low variation (Figure 3C, D, F). Other results were shown with those of *A. cerana* from the Moluccas, and *A. nigrocincta* from Sulawesi have several displacements in the landmark 8, 9, and 10 were shown in the deformations grid (Figure 3E, G).

At the interspecies level in *A. cerana* and *A. nigrocincta*, landmarks 11, 16, and 17 showed the highest contribution value (Table 6). This result means that the three landmarks contributed to the most displacements among the 19 landmarks in these two cavity-nesting bees among the six islands (Table 6) and revealed a different wing form based on grid deformation between two species (Figure 6). The interspecies result has shown that *A. nigrocincta* has higher bending energy than *A. cerana* (Table 7). Our

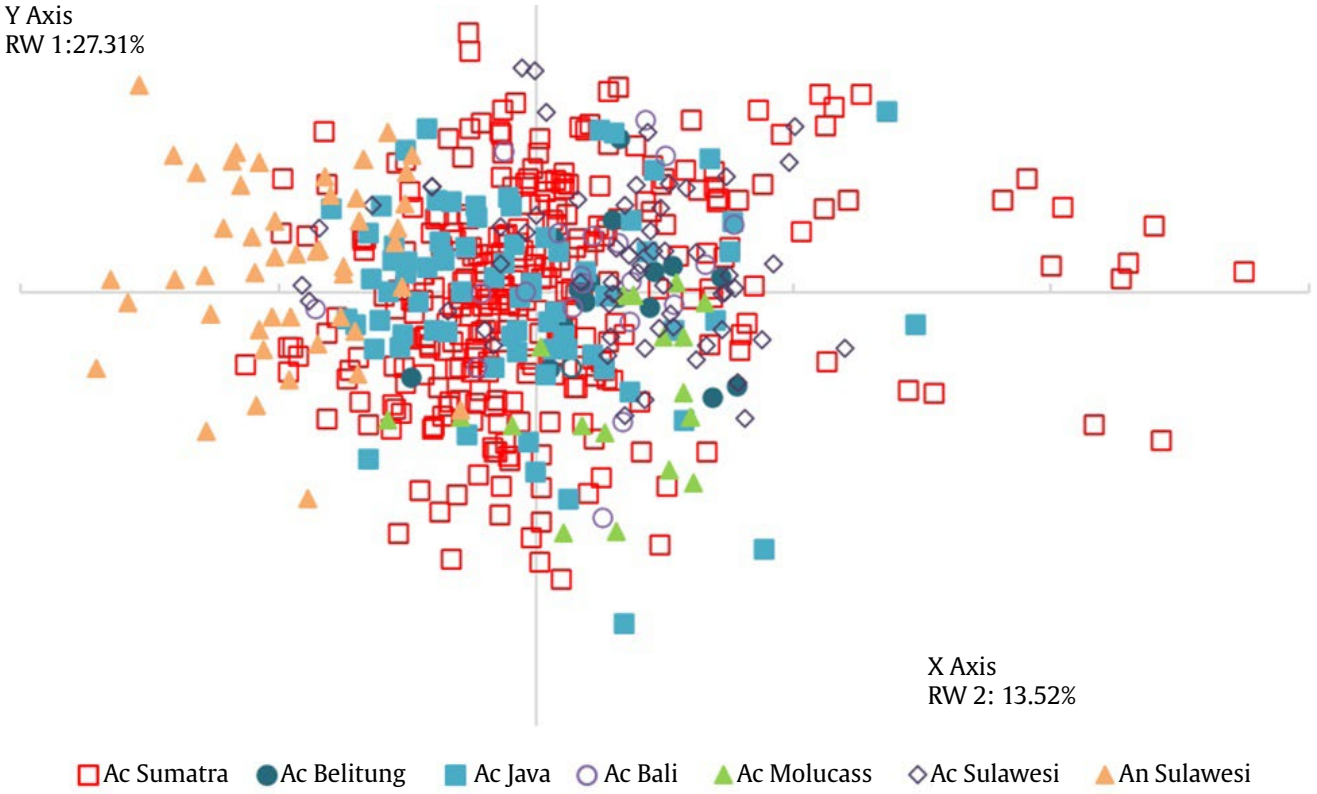

Figure 4. Principal component analysis of *A. cerana* and *A. nigrocincta* 550 worker honey bees from six islands in Indonesia measured for 19 anatomical landmarks

geometric morphometric study can distinguish *A. cerana* and *A. nigrocincta* based on shape deformation and bending energy value.

3.3. The Relationship of *A. cerana* and *A. nigrocincta* Based on Principal Component Analysis (PCA) and Dendrogram

The relative warp cumulative from the 550 individuals of *A. cerana* and *A. nigrocincta* were constructed and revealed 40.83% scores of the RW 1 and RW 2 in the plot ordination (Figure 4). All samples of *A. cerana* were spread in the PCA plots; the Sumatra, Java, and Sulawesi samples were scattered through all quadrants and had considerable overlap. However, *A. cerana* Belitung and the Moluccas were spread in quadrants two and three, respectively. Quadrant one and four showed an interspecies level that *A. nigrocincta* appeared to group separately (Figure 4).

The cluster of *A. cerana* and *A. nigrocincta* was described by a rooted and unrooted NJ dendogram tree (Figure 5 and 7). Intraspecies *A. cerana* revealed three significant clusters that appeared closely related to geographical locations on each island. *Apis cerana* Java and Sumatra spread in all clusters, while *A. cerana* from Sumatra and Belitung clustered in the same clade. On the other hand, *A. cerana* Java and the Moluccas have a close relationship, at the same time, *A. cerana* Sulawesi is also similar to *A. cerana* Java (Figure 5). In addition, an unrooted NJ tree was constructed to explain the relationship in interspecies variations of *A. cerana* and *A. nigrocincta* and confirmed using geometric morphometrics that *A. nigrocincta* is a separated clade *A. cerana* (Figure 7).

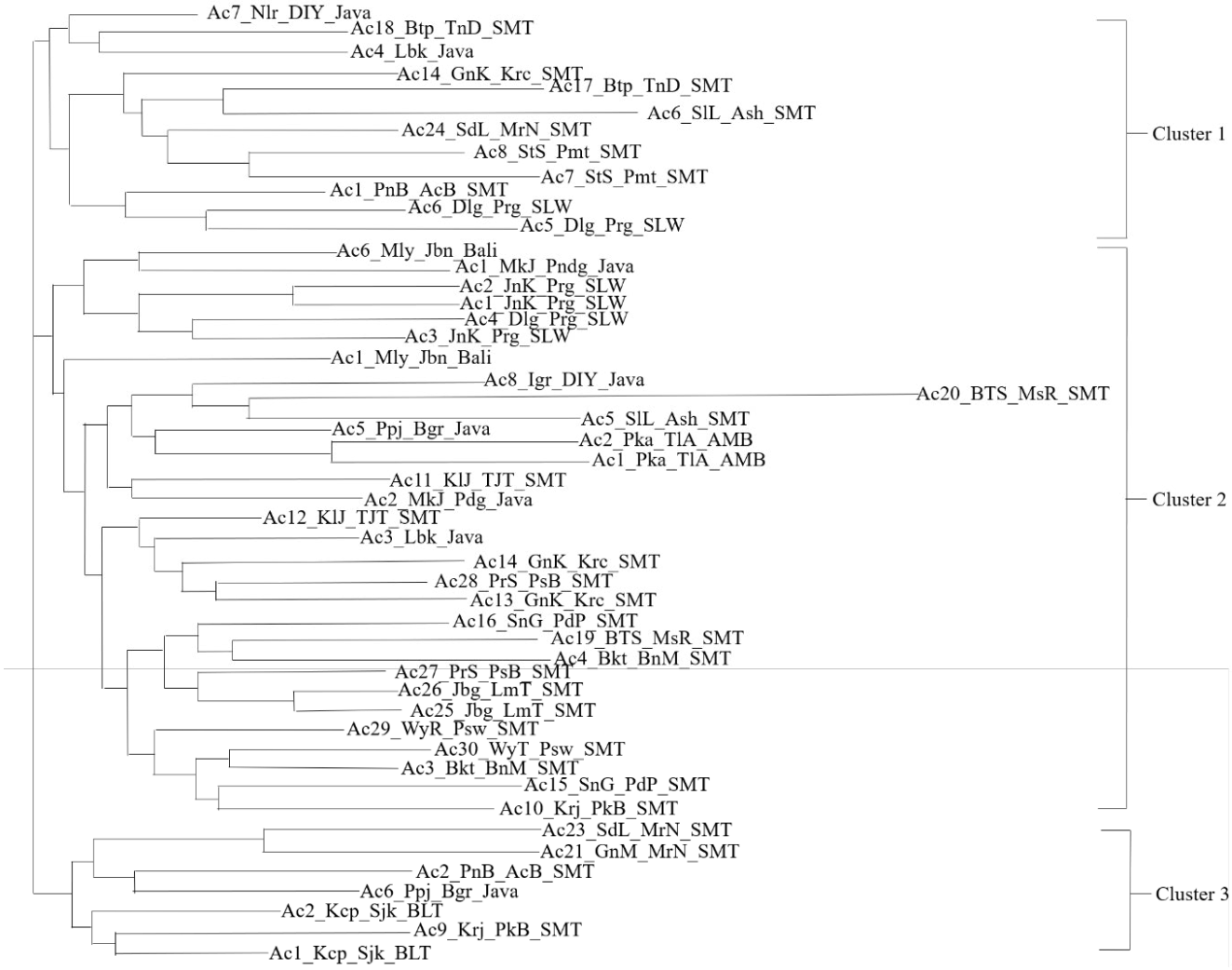

Figure 5. Neighbor-joining rooted phylogenetic tree of *A. cerana* based on 50 colonies in each island. Abbreviation of the OTUs refers to Table 1

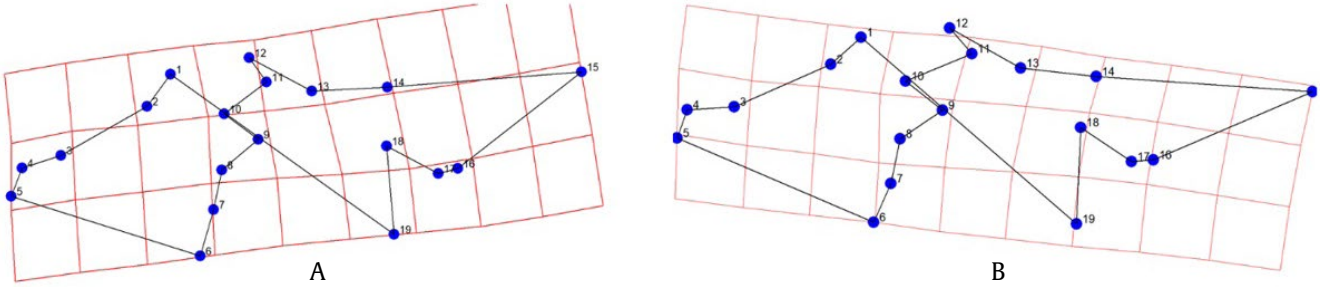

Figure 6. Deformation grid of wing venation all 500 individuals *A. cerana* were aligned to the mean landmark of *A. nigrocincta* (A) and all 50 individuals *A. nigrocincta* aligned to the mean landmark of *A. cerana* (B). Note: the straight and unbent grid refers to the exact shape to reference a landmark. The more bending to the box indicates the sample has a more different shape to the reference

Table 6. Landmark contribution values of the total 55 colonies of *A. cerana* and *A. nigrocincta*

Landmark	Contribution value	S^2
1	0.03247	0.00001215
2	0.03145	0.00001057
3	0.01927	0.00000908
4	0.05140	0.00001203
5	0.02031	0.00001782*
6	0.01283	0.00001473
7	0.05909	0.00001147
8	0.05965	0.00000719
9	0.03525	0.00000835
10	0.03682	0.00001530
11	0.12551*	0.00001285
12	0.05532	0.00001289
13	0.02869	0.00001283
14	0.00735	0.00001666*
15	0.00035	0.00003030*
16	0.15877*	0.00001325
17	0.24034*	0.00001014
18	0.02324	0.00001389
19	0.00189	0.00001506

*The most contribution and variation of landmarks values that have high variations

Table 7. Bending energy and Procrustes distance values *A. cerana* and *A. nigrocincta*

Species	Bending energy	Procrustes distance (d)
A. cerana	0.04185	0.04381
A. nigrocincta	0.04439	0.04381

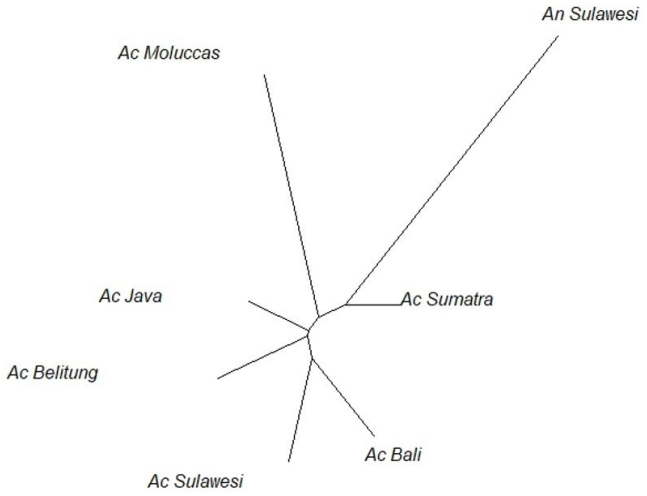

Figure 7. Neighbor-joining unrooted phylogenetic tree of *A. cerana* (Ac) and *A. nigrocincta* (An) in six islands

4. Discussion

Geometric morphometrics has been applied to the landmark wing venations and successfully discriminates many insect species, especially in honey bees (Combey *et al.* 2018). The two cavity-nesting honey bees, *A. cerana* and *A. nigrocincta* were distinguished based on 19 landmarks coordinates of wing venation. The landmarks displacement in wing venation of interspecies affected bending energy (Table 7). It revealed a different deformation grid of *A. nigrocincta* Sulawesi and *A. cerana* Sumatra, Belitung, Java, Bali, Sulawesi, and Moluccas (Figure 6A and B). This result showed that those two species have different wing shapes (Figure 6A and B). Our result is in concordance with the previous study that different wing shapes from other *Apis* species have a variety of deformation grids (Santoso *et al.* 2018). Honey bee *A. andreniformis, A. cerana*, and *A. dorsata* showed a different deformation grid based on 19 landmarks displacement in the interspecies level (Santoso *et al.* 2018).

Wing landmarks venations are essential coordinates reflecting size, shape, location, and orientation (Cooke and Terhune 2015). Landmarks of 11, 16, and 17 have a high contribution value and are the marker landmarks in the interspecies level of *A. cerana* and *A. nigrocincta*, as well as in the intraspecies level of *A. cerana* (Table 6). In agreement with this result, *A. cerana* from three sample locations in China significantly contributed to landmarks number 2, 3, and 5 (Zhou *et al.* 2016). Those landmark numbers are the same as the landmark of 11, 16, and 17 of this study. The two landmarks contribution number 16 and 17 have the highest variations (Table 6), which in the traditional morphometric analysis is known as cubital index (CI) character of ratio a/b (Ruttner 1988). The cubital index has been long known as a character of the species of *Apis*, such as the high a/b ratio of *A. koschevnikovi* wing venation compared to the sympatric *A. cerana* Kalimantan (Hadisoesilo *et al.* 2008). *Apis cerana* from Bajaura, India, has a minimum cubital index (2.70 mm) compared to *A. cerana* from Bharmour, Nagrota Bagwan, Palampur, and Sangla based on traditional morphometric (Ibrahim *et al.* 2019). The traditional morphometric methods showed that *A. mellifera* in Turkey from Kõrklareli and Austria have a similarity in the cubital index (Kandemir *et al.* 2005). The cubital index also differentiates subspecies *A. mellifera* mellifera, *A. m. ligustica, A. m. carnica*, and *A. m. carnica* showed the highest cubital index value in subspecies wing characters (Keller *et al.* 2014).

The landmark displacement of wing venations influenced the bending energy value at the interspecies level and showed that *A. nigrocincta* has higher landmark variations than *A. cerana* (Table 7). Our finding supports that *A. nigrocincta* are morphologically different from *A. cerana* in Sulawesi, which has been proven by the presence of

a yellow colour difference in the morphology of *A. nigrocincta* (Hadisoesilo *et al.* 1995) and revealed 85% significantly different in morphological characters based on PCA analysis (Nur'aini and Purwanto 2021).

The geographical locations based on six islands of *A. cerana* showed the similarity of *A. cerana* from Sulawesi and Moluccas to reference landmarks. This result was supported by PCA that showed *A. cerana* from Sulawesi are clustered with Sumatra and Java to the centroid (Figure 4). The PCA agrees with the Neighbor-Joining tree that revealed *A. cerana* from Moluccas and Sulawesi is closely related to *A. cerana* from Java (Figure 5). This result is possible due to the introduction of *A. cerana* from Java to Moluccas (Maa 1953) and Sulawesi (unpublished data). *Apis cerana* Moluccas sample (Poka village, Ambon) is also confirmed based on the molecular markers of *COX1*, *COX2*, *IGS*, and *mrjp2* genes are in the same clade with *A. cerana* Java (Parung Panjang, Bogor) (Raffiudin *et al.* 2021). A close relationship was also found among 180 individuals *A. cerana* in China from three sites, i.e., Jilin, Hainan, and Shaanxi), that showed an overlapping group for all samples (Zhou *et al.* 2016).

Although the PCA and Neighbor-Joining analysis showed the overlapping between *A. cerana* in different islands, the study based on bending energy can differentiate intraspecies *A. cerana* in Sumatra by the altitudes. *Apis cerana* from lowland North Sumatra and Jambi revealed lower bending energy than the highland samples (Table 4). The same phenomena were also shown in the different altitudes of *A. mellifera* in Pantanal, Brazil, which produced a slight wing venation variation in the geometric morphometric analysis (Peil and Aranda 2021). Another study based on traditional morphometric character showed that *A. cerana* from the highland Philippines differed clearly from the lowland (Tilde *et al.* 2000). This differentiation is plausible due to the higher temperature in the lowlands compared to the highland. The temperature indirectly affects morphological size variations in worker bumblebees species *Bombus impatiens* (Kelemen and Dornhaus 2018). Furthermore, honey bee *A. cerana* has a relatively long survival rate at 35°C with 50% humidity (Li *et al.* 2019). The environmental factors affect the adaptation and survival of species; moreover, this phenomenon can be affected to the functional morphology such as wing (Willmore *et al.* 2007).

Based on landmark wing venation, the PCA and Neighbor-Joining revealed that ten individuals *A. cerana* from the lowland of Musi Rawas (South Sumatra) were more discrete to the centroid of the cartesian coordinate (Figure 4). The deviation of plot ordination was also found in Canonical Variate Analysis (CVA) based on landmark and wing shape of *A. mellifera* from Iran and showed that the honey bee population from Tarom was separated based on eight shapes variable on the hind wing (Dolati *et al.* 2013). The separated plot on PCA analysis from several individuals of *A. cerana* in Musi Rawas (South Sumatra) indicates the distinct shape; thus, other morphological characters and molecular markers are needed to justify further the subspecies status of the lowland *A. cerana* Musi Rawas.

According to our results, although the distribution based on intraspecies *A. cerana* in Sundaland and Wallacea showed differences in the grid deformations, however, they are originated from the same resource in six islands. These phenomena were shown in the geometric morphometric presented in PCA and the Neighbor Joining tree. This research has revealed that geometric morphometric is a specific and simple method for identifying honey bee species found on intraspecies with different altitudes, intraspecies from various islands, and differentiation in interspecies.

In conclusion geometric morphometric has successfully shown intraspecies variations of *A. cerana* from Sumatra, Belitung, Java, Bali, Sulawesi, and the Moluccas in landmarks 11, 16, and 17. The highest variation was seen in *A. cerana* Sumatra, with the highest bending energy. Bending energy is also proven to group *A. cerana* Sundaland and Wallacea, influenced by landmarks 16 and 17, known as cubital index landmarks. The differences of wing venations between *A. cerana* and *A. nigrocincta* show a distinct branch based on unrooted Neighbor-Joining, also supported by separation plots in PCA.

Acknowledgements

We acknowledged the Ministry of Research and Technology/National Research and Innovation Agency (Indonesia) for the grant to the corresponding author entitled "Evolution of honeybee *Apis cerana* in Indonesia: Morphology and Molecular Approach" (No: 1/E1/KP.PTNBH/2021). We are grateful to Nagao Environmental Foundation that partly funded this research entitled: "Distribution and molecular approach of the Sulawesi endemic honey bee species *Apis nigrocincta*". Our appreciation also goes to the bee farmers that give support during *Apis cerana* collections.

References

Combey, R., Quandahor, P., Mensah, B.A., 2018. Geometric morphometrics captures possible segregation occurring within subspecies *Apis mellifera* adansonii in three agro ecological zones. *Ann. Biol. Res.* 9, 31-43.

Cooke, S.B., Terhune, C.E., 2015. Form, function, and geometric morphometrics. *Anat. Res.* 298, 5-28. https://doi.org/10.1002/ar.23065

Damus, M.S. Otis, G.W., 1997. A morphometric analysis of *Apis cerana* F and *Apis nigrocincta* Smith populations from Southeast Asia. *Apidologie*. 28, 309–323. https://doi.org/10.1051/apido:19970507

Dolati, L., Rafie, J.N., Khalesro, H., 2013. Landmark-based morphometric study in the fore and hind wings of an Iranian race of European honeybee (*Apis mellifera* meda). *J. Apic. Sci.* 57, 187-197. https://doi.org/10.2478/jas-2013-0028

Engel, M.S., 1999. The taxonomy of recent and fossil honey bees (Hymenoptera: Apidae; *Apis*). *J. Hymenopt. Res*. 8, 165–196.

Hadisoesilo, S., Otis, G.W., Meixner, M., 1995. Two distinct populations of cavity-nesting honey bees (Hymenoptera: Apidae) in South Sulawesi. *J. Kansas Entomol Soc.* 68, 399–407.

Hadisoesilo, S., Raffiudin, R., Susanti, W., Atmowidi, T., Hepburn, C., Radloff, S. E., Hepburn, H. R., 2008. Morphometric analysis and biogeography of *Apis koschevnikovi* Enderlein (1906). *Apidologie*. 39, 495-503. https://doi.org/10.1051/apido:2008029

Ibrahim, M.M., Chandel, Y.S., Anil, 2019. Morphometrics of *Apis cerana* from agroclimatic zones of Himachal Pradesh. Indian. *J. Entomol.* 81, 406-410. https://doi.org/10.5958/0974-8172.2019.00116.0

Ji, Y., Li, X., Ji, T., Tang, J., Qiu, L., Hu, J., Zhou, X., 2020. Gene reuse facilitates rapid radiation and independent adaptation to diverse habitats in the Asian honeybee. *Sci. Adv*. 6, 1-14. https://doi.org/10.1126/sciadv.abd3590

Kandemir, I., Kence, M., Kence, A. 2005. Morphometric and electrophoretic variation in different honeybee (*Apis mellifera* L.) populations. *Turkish J. Vet. Anim. Sci*. 29, 885-890.

Keller, E. M., Harris, I., Cross, P. 2014. Identifying suitable queen rearing sites of Apis mellifera mellifera at a regional scale using morphometrics. *J. Apic. Res*. 53, 279-287.

Kelemen, E., Dornhaus, A. 2018. Lower temperatures decrease worker size variation but do not affect fine-grained thermoregulation in bumble bees. *Behav. Ecol. Sociobiol.* 72, 1-8.

Li, X., Ma, W., Shen, J., Long, D., Feng, Y., Su, W., Jiang, Y. 2019. Tolerance and response of two honeybee species *Apis cerana* and *Apis mellifera* to high temperature and relative humidity. *PLoS ONE* 14, e0217921.

Maa, T.C., 1953. An inquiry into the systematics of the tribus Apidini or honeybees (Hym.). *Treubia*. 21, 525-640.

Michener, C.D., 2007. The Bees of the World, second ed. John Hopkins University Press, Baltimore.

Nuraini, N., Purwanto, H., 2021. Morphology, morphometrics, and molecular characteristics of *Apis cerana* and *Apis nigrocincta* from Central Sulawesi, Indonesia. *J. Biol. Tropis*. 21, 368-382. https://doi.org/10.29303/jbt.v21i2.2614

Otis, G.W., 1996. Distributions of recently recognized species of honey bees. *J. Kansas. Entomol. Soc.* 69, 311–333.

Paradis, E., Claude, J., Strimmer, K., 2004. APE: analyses of phylogenetics and evolution in R language. *Bioinformatics*. 20, 289-290. https://doi.org/10.1093/bioinformatics/btg412

Peil, A.C., Aranda, R., 2021. Potential niche modeling distribution and wing geometric morphometrics of *Apis mellifera* in the Brazilian Pantanal. *Sociobiology*. 68, e5629. https://doi.org/10.13102/sociobiology.v68i2.5629

R Core Team., 2018. R: A Language and Environment for Statistical Computing. R Foundation for Statistical Computing, Vienna. Available at: https://www.R-project.org/. [Date accessed: 10 January 2020]

Radloff, S.E., Hepburn, C., Hepburn, H.R., Fuchs, S., Hadisoesilo, S., Tan, K., Kuznetsov, V., 2010. Population structure and classification of *Apis cerana*. *Apidologie*. 41, 589-601. https://doi.org/10.1051/apido/2010008

Raffiuddin, R., Sosromarsono, S., Ratna, E.S., Solihin, D.D., 1999. Morphological variation of the asian honeybee *Apis cerana* (f) (Hymenoptera: Apidae) in West Java. *Bul. HPT. IPB*. 11, 20–25.

Raffiudin, R., Crozier, R.H., 2007. Phylogenetic analysis of honey bee behavioral evolution. *Mol. Phylogenet. Evol.* 43, 543–552. https://doi.org/10.1016/j.ympev.2006.10.013

Raffiudin, R., Shullia, N.I., Damayanti, A.U., Wahyudi, D.T., Febiriani, T.V., Atmowidi, T., Lamerkabel, J.S., Widjaja, M.C., 2021. New haplotypes of *Apis cerana* in Indonesia: identification from mitochondrial and *mayor royal jelly protein 2 genes. Int. J. Trop. Insect. Sci*. DOI:10.1007/s42690-021-0055-x

Rattanawannee, A., Chanchao, C., Wongsiri, S., 2010. Gender and species identification of four native honey bees (Apidae: *Apis*) in Thailand based on wing morphometic analysis. *Ann. Entomol. Soc. Am*. 103, 965-970. https://doi.org/10.1603/AN10070

Rohlf, F.J., Slice, D., 1990. Extensions of the procrustes method for the optimal superimposition of landmarks. *Syst. Biol*. 39, 40-59. https://doi.org/10.2307/2992207

Rohlf, F.J., 1993. Relative Warp Analysis and An Example of Its Application to Mosquito Wings, first ed. Stony Brook, New York.

Rohlf, F.J., Loy. A., Corti, M., 1996. Morphometric analysis of old world Talpidae (Mammalia, Insectivora) using partial-warps scores. *Syst. Biol*. 45, 344-362. https://doi.org/10.1093/sysbio/45.3.344

Rohlf, F.J., 2015. The tps series of software. *Hystrix*. 26, 1-4.

Rohlf, F. J., 2004. TpsSpline, Thin-Plate Spline, Version 1.20, first ed. Stony Brook, New York.

Ruttner, F., 1988. Biogeography and Taxonomy of Honeybees, first ed. Springer Verlag, Berlin. https://doi.org/10.1007/978-3-642-72649-1

Santoso, M. A. D., Juliandi, B., Raffiudin, R., 2018. Honey bees species differentiation using geometric morphometric on wing venations. *In: IOP Conference Series: Earth and Environmental Science, Vol. 197*. Bogor: IOP Publishing. pp. 1-7. https://doi.org/10.1088/1755-1315/197/1/012015

Tilde, A.C., Fuchs, S., Koeniger, N., Cervancia, C.R., 2000. Morphometric diversity of *Apis cerana* Fabr. within the Philippines. *Apidologie*. 31, 249-263. https://doi.org/10.1051/apido:2000120

Tofilski, A., 2008. Using geometric morphometrics and standard morphometry to discriminate three honeybee subspecies. *Apidologie*. 39, 558–563. https://doi.org/10.1051/apido:2008037

Willmore, K. E., Young, N. M., Richtsmeier, J. T. 2007. Phenotypic variability: its components, measurement and underlying developmental processes. *Evol. Biol.* 34, 99-120.

Zelditch, M.L., Swiderski, D.L., Sheets, H.H., 2004. Geometric Morphometrics for Biologists: A Primer, second ed. Academic Press, London.

Zhou, S., Zhu, X., Xu, X., Zheng, X., Zhou, B., 2016. Assessing of geometric morphometrics analyses in microtaxonomy of the *Apis cerana* Fabricius (Hymenoptera: Apidae) within China. *J. Kansas. Entomol. Soc.* 89, 297-305. https://doi.org/10.2317/0022-8567-89.4.297